

Influence of Cl^- , Br^- , NO_3^- and SO_4^{2-} ions on the corrosion behaviour of 6061 Al alloy

J DATTA*, C BHATTACHARYA and S BANDYOPADHYAY†

Department of Chemistry, B.E. College (D.U.), Howrah 711 103, India

†School of Materials Science & Engineering, University of New South Wales, Sydney, Australia

MS received 7 April 2004; revised 4 March 2005

Abstract. The effects of anions like Cl^- , Br^- , NO_3^- and SO_4^{2-} on the anodic dissolution of the monolithic Al 6061 alloy have been investigated at neutral pH through immersion testing and electrochemical techniques like potentiodynamic polarization and a.c. impedance spectroscopy. Scanning electron microscopy was employed to characterize the corroded surface and to observe the extent of pitting in different media. From the evaluated corrosion parameters it was found that the dissolution of the matrix was extensively reduced in presence of aqueous solutions containing Br^- , NO_3^- and SO_4^{2-} ions while Cl^- ions aggravated corrosion by penetrating into the barrier oxide film on the surface of the material. Pronounced effect of pitting was observed in presence of Cl^- and the level of pitting in NO_3^- and Br^- were mild. In presence of SO_4^{2-} ions passivity was extended over a wide potential range and breakdown of passivity occurs when the material was polarized beyond pitting potential. The departure of capacitive behaviour towards resistive behaviour was clearly observed through impedance measurements when investigations were conducted in Cl^- media and in presence of the other electrolytes. Corrosion rates were, however, controlled during prolonged exposure in the electrolytic media, specially in case of chloride media, due to the predominance of film repair kinetics.

Keywords. Alloys; corrosion test; scanning electron microscopy (SEM); electrochemical properties.

1. Introduction

In recent years the environmental factors affecting the corrosion behaviour of aluminium and its alloys have very often been studied (Bohni and Uhlig 1969; Stella and Micheli 1978; Ambat and Dwarakadasa 1994; Guillaumin and Mankowski 2000; Kotsikos *et al* 2000). Particularly, the low density alloys in course of widespread application are frequently exposed to saline and other electrolytic media and have been the subject of corrosion studies. The monolithic Al 6061 alloy has recently been the attractive matrix alloy for the fabrication of ceramic particles reinforced composites that offer the prospect of materials with high stiffness and make them useful to aerospace industries (Das *et al* 1996). In our previous work non-reinforced Al 6061 alloy showed susceptibility towards corrosion in acidic and quite distinctively in alkaline medium whereas it was found to be relatively corrosion resistant at neutral pH (Datta *et al* 2003). In the present paper we have studied the corrosion behaviour of the same alloy in aqueous medium at neutral pH in presence of different electrolytes such as NaCl, NaBr, NaNO_3 and Na_2SO_4 . The investigations were conducted through electrochemical polarization technique, electrochemical impedance spectro-

scopy (EIS), immersion testing and subsequent microscopic analysis in scanning electron microscope (SEM). The objective of the present investigation is to study the corrosion behaviour of the as received Al 6061 alloy under exposure to the said electrolytes and correlate the measured corrosion rates with the relative extent of pits and cracks developed on the surface of the material as observed from electron microscopy.

2. Experimental

All the materials were provided in the form of 19 mm diameter extruded rods by Comalco Research Centre (CRC), Thomastown, Australia. The monolithic alloy Al 6061 was direct-chill-cast at CRC and then hot extruded (Das *et al* 1996). The composition of the alloy used was determined using CAMECA SX50 electron probe micro-analyser and is given in table 1. The as-received alloy samples were cut in the form of coupons and polished on one side using emery paper (1–6) for corrosion measurements in 0.1 M solutions of various electrolytes (all of E-Merck, AR grade) such as NaCl, NaBr, NaNO_3 and Na_2SO_4 . Double distilled water at pH 6–7 was used to prepare the solutions.

2.1 Immersion tests

Coupons with exposed area of 1 sq cm were kept immersed in the working solutions for 2–15 days. The experi-

*Author for correspondence (jayati_datta@rediffmail.com; jayatidatta@chem.becs.ac.in)

Table 1. Chemical composition of the 6061 aluminium alloy.

Materials	Chemical composition (wt%)							
	Mg	Si	Fe	Cr	Cu	Mn	Ti	Al (balance)
6061	0.690	0.549	0.022	0.065	0.168	0.094	0.017	98.835

Table 2. Electrochemical corrosion parameters of Al 6061 in 0.1 M solutions of different electrolytes at pH 6.7.

Corrosion parameters	NaCl	NaNO ₃	NaBr	Na ₂ SO ₄
E_{corr} /mV vs SCE	-590	-500	-731	-600
I_{corr} /A m ⁻²	0.06	0.028	0.028	0.016
Corr. rate/mm yr ⁻¹	0.06	0.03	0.03	0.016

mental samples were weighed before immersion in solutions for stipulated time. To observe pitting effect the final weight of the samples were taken after removing precipitates adhered on the surface of the materials with nylon brush, cleaning in a solution containing 5 ml chromic acid and 30 ml 85% phosphoric acid per litre and finally rinsing in double distilled water as described in ASTM-G-1-72 (ASTM Standards Annual Book 1977).

2.2 Polarization studies in aerated conditions

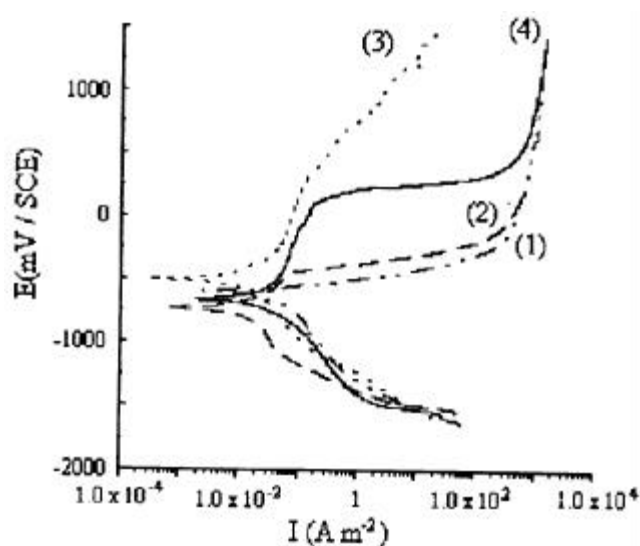
Linear sweep voltammetry (potentiodynamic polarization) was performed on the samples (exposed area of 1 sq cm at the scan rate of 1 mV s⁻¹) within the potential range of -1500 mV to 1000 mV vs SCE (W) in all the working solutions in a three-electrode assembly cell as described earlier (Datta *et al* 2004) and measurements were made by AUTOLAB 30 Potentiostat-Galvanostat, The Netherlands.

2.3 Microscopic analysis

Following the immersion and polarization tests, the samples were subjected to SEM analysis after usual pretreatment (ASTM Standards Annual Book 1977). The micrographs were taken in JEOL 840 SEM.

2.4 EIS studies in aerated conditions

AC impedance spectra for the 6061 Al alloy were obtained using a frequency response analyser (FRA) combined with the AUTOLAB 12 PG Stat. EIS measurements were conducted at open circuit conditions after a steady state potential was attained in aerated 0.1 M solution of different electrolytes at neutral pH. The experiment was performed in a three-electrode one compartment cell containing the test coupons as working electrode, a large area Pt foil as

**Figure 1.** Potentiodynamic polarization curves (0.1 M solutions of different salts under aerated medium at a scan rate of 1 mV s⁻¹. ((1) NaCl, (2) NaBr, (3) NaNO₃ and (4) Na₂SO₄).

counter electrode and a saturated calomel reference electrode. An a.c. sinusoidal perturbation of 5 mV r.m.s. was applied at the cell open circuit potential over the frequency range of 100 kHz to 20 mHz, in 50 steps. Data fitting to equivalent circuit were performed with the associated software.

3. Results and discussion

Typical polarization curves for the material in salt solutions containing Cl⁻, Br⁻, NO₃⁻ and SO₄²⁻ at pH 6.7 in aerated conditions are shown in figure 1. The evaluated corrosion parameters are given in table 2. The salts of Br⁻ and NO₃⁻ are found to be less aggressive to the alloy showing relatively less corrosion rates than the Cl⁻ salts.

Anodic dissolution of the Al alloy as Al^{3+} is, therefore, pronounced in solution containing Cl^- . This presumably indicates less solubility of the Al^{3+} complexes formed in these electrolytes without Cl^- ions (Greenwood and Earnshaw 1989). As shown in figure 1, defined passive regions appeared in the media containing SO_4^{2-} ions which are, however, absent in NaCl solution and others at neutral pH.

Distinct matrix loss by corrosion was detected in each of the immersion medium as indicated by the weight loss data. For each of the immersion period the corrosion rates of the material were evaluated using traditional equation (Fontana 1987). The weight loss (in mg cm^{-2}) during immersion in each of the solutions were plotted against duration of immersion as shown in figure 2. The immersion data including weight loss and average corrosion rate (in mm yr^{-1}) for the material in working solutions as obtained from the slope of the plot are summarized in table 3. Corrosion rates are found to increase with increasing period of immersion. The relative degree of corrosion in presence of different ionic species is in the order $\text{Cl}^- > \text{NO}_3^- \geq \text{Br}^- > \text{SO}_4^{2-}$ and corroborates with the order obtained from electrochemical studies. Notably, with prolonged immersion in solutions containing ions other than Cl^- , the

increasing trend of weight loss is found to be suppressed to some extent. The maximum corrosion rate in presence of chloride ions is indicative of the high penetrating power of these aggressive ions into the barrier oxide film as well as their ability to retard the film repair kinetics in the experimental condition (Tomcsanyi *et al* 1989). With an approximately equivalent activity (the prepared working solutions are of 0.1 M for each of the electrolytes), the Br^- and NO_3^- ions are found to deteriorate the material to a less extent as shown from the moderate weight loss in presence of these salts.

During immersion testing in most of the electrolytes, surface of the materials were grown with some amount of solid products. Some of these test samples were subjected to SEM studies that indicated possible formation of oxides and other products adhered to the surface during corrosion. Scanning electron micrograph for the as received sample is presented in figure 3 for comparison with the corroded ones. Figure 4 is representative of SEM, at higher magnification, which shows cracked and pit initiated areas of the sample after immersion for 72 h in 0.1 M NaCl solution. Aggressive attack by chloride ions was observed throughout the surface. SEM of samples immersed in 0.1 M solutions of Br^- and SO_4^{2-} for 72 h were presented in figures 5 and 6 showing very few pits on the surfaces as compared to that in the chloride medium. Under extended immersion period of 7 days (168 h) in medium containing NO_3^- , pits on the surfaces were found to be elongated and grown in size as shown in a typical micrograph (figure 7). Similarly, a typical picture of the microscopic tunneling in pit-initiated area on the surface exposed for prolonged duration of 15 days (360 h) in 0.1 M NaCl solution was shown in figure 8.

On the other hand sulfate ion in the medium appears to impart passivity to the alloy as observed from the decreased weight loss (figure 2) and reduced corrosion rates (table 2). In fact, the presence of SO_4^{2-} in the medium is likely to produce aluminium sulfates which are less soluble than the other Al salts formed in presence of Br^- , NO_3^- and Cl^- and may effectively retard the surface degradation by delaying the onset of pitting (Pyun *et al* 1999). However, when the sample was polarized in 0.1 M Na_2SO_4 solution, it showed appreciable amount of pitting apparently due to breakdown of passivity beyond pitting potential (225 mV). Large pits were observed (figure 9)

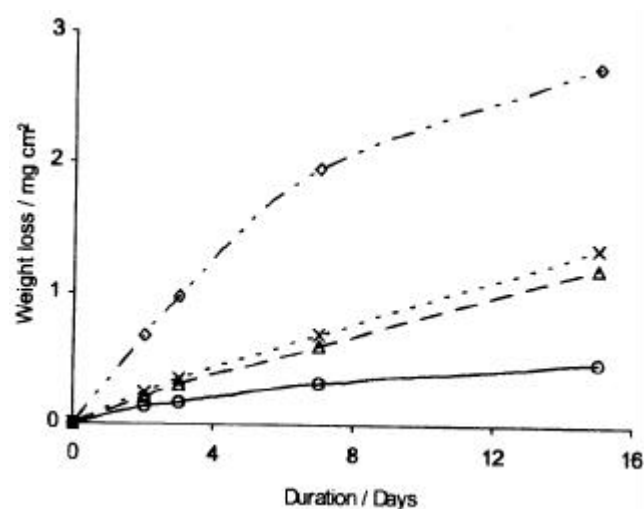


Figure 2. Variation of weight loss (mg cm^{-2}) with duration of immersion [— - □ —, NaCl; —△—, NaBr; - - × - -, NaNO_3 and —○—, Na_2SO_4].

Table 3. Results of immersion studies in different electrolytes for different periods at 25°C.

Solutions (0.1 M)	2 Days	3 Days	7 Days	15 Days	Average corrosion rate (mm yr^{-1})
	Wt. loss/mg cm^{-2}	Wt. loss/mg cm^{-2}	Wt. loss/mg cm^{-2}	Wt. loss/mg cm^{-2}	
NaCl	0.68	0.98	1.96	2.74	0.28
NaNO_3	0.24	0.36	0.72	1.45	0.14
NaBr	0.20	0.30	0.60	1.20	0.10
Na_2SO_4	0.13	0.16	0.32	0.48	0.05

on the surface with corrosion products, presumably sulfates of aluminium.

The above chemical and electrochemical investigations were further supported by EIS measurements. The influence of different anions on impedance spectra of the alloy is shown in Nyquist and Bode plots (figures 10 and 11). In the Nyquist plots (figure 10), capacitive semicircles are obtained with different diameters for different electrolytes. It is well known that high frequency capacitive semicircles are related to the dielectric properties and thickness of the barrier film and the low frequency inductive loops are indicative of the specific adsorption of anions (McCafferty 2003). Incomplete inductive loops are often visible which suggest occurrence of localized corrosion in certain media (Chavanin 1991; Metikos-Hukovic *et al* 1994).

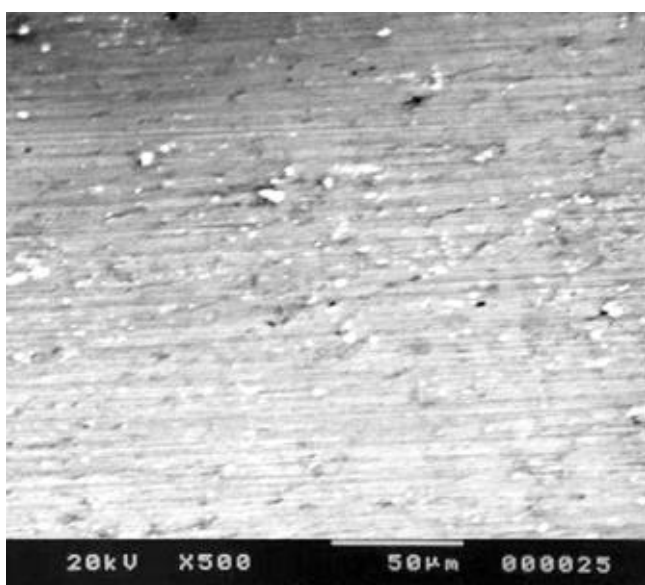


Figure 3. Micrograph of the non-corroded 6061 Al sample.

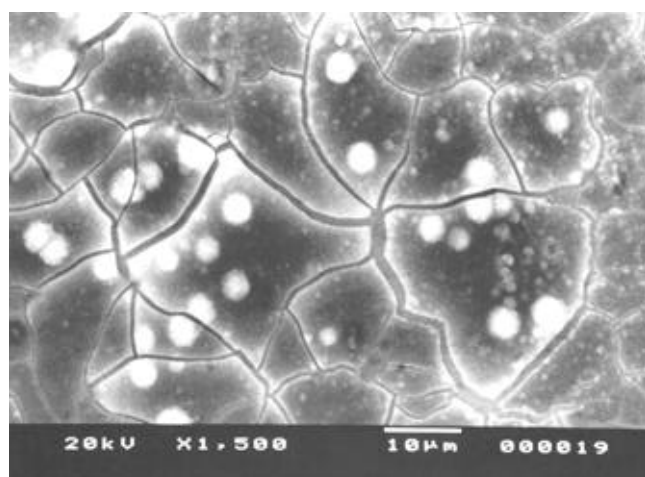


Figure 4. Micrograph of the sample immersed in 0.1 M NaCl solution for 3 days.

In the present investigation, well defined capacitive semicircle (figure 10) in case of Cl^- ions suggests that the corrosion process occurs under activation control (Conde and Damborenea 1998). Further, the incomplete inductive loop is likely to reflect specific adsorption of Cl^- and sequential localized corrosion by the attack of aggressive Cl^- ions into the barrier film. However, specific adsorption on the oxide layer by the anions like Br^- , SO_4^{2-} and NO_3^- is unfavourable as indicated by the absence of inductive loop in the Nyquist plots (figure 10), although localized corrosion is found in some cases.

In the Bode plot (figure 11), it is observed that the maximum phase shift, q_{max} , in different media are in the order of $\text{Cl}^- > \text{Br}^- > \text{SO}_4^{2-} \approx \text{NO}_3^-$. The inductive behaviour in chloride solution caused by the localized process is apparent as the impedance decreases at low frequencies. The difference between the high frequency limit and low

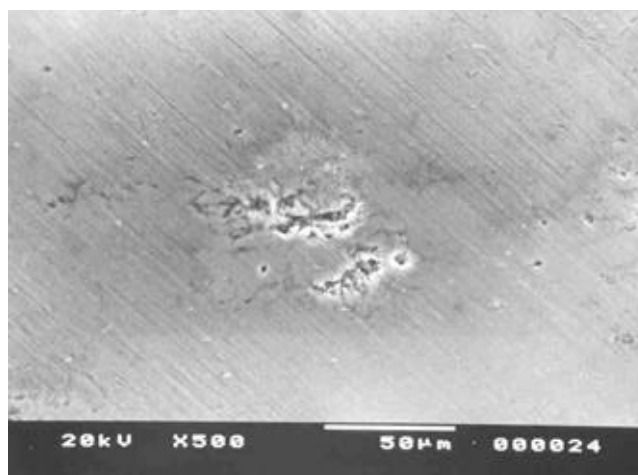


Figure 5. Micrograph of the sample immersed in 0.1 M NaBr solution for 3 days.



Figure 6. Micrograph of the sample immersed in 0.1 M Na_2SO_4 solution for 3 days.

frequency limit in the Bode plot is equal to R_p , the polarization resistance, which is associated with the dissolution and repassivation processes occurring at the interface as well as with the electronic conductivity of the film. R_p is significantly lowered in case of Cl^- ion due to its penetration power through the barrier oxide film and direct contact with the matrix. However, when the NO_3^- and SO_4^{2-} ions approach the surface they seemingly get adsorbed in the voids of the oxide film through p -bonding with the metal oxide.

The above impedance data have been analysed based on the simple Randles equivalent circuit (EC) model as represented in figure 12. The circuit includes a solution resistance (R_s), a charge transfer or polarization resistance (R_p) and a constant phase element (CPE), which substitutes the double layer capacitance for the film. CPE takes into account the phenomena related to the heterogeneous nature of surface and diffusion processes (McDonald 1987; Kahanda and Tomkiewicz 1990). The

evaluated EC parameters are summarized in table 4. The R_p values in different electrolytes for the alloy material are found to be in the order of $\text{NO}_3^- > \text{SO}_4^{2-} > \text{Br}^- > \text{Cl}^-$.

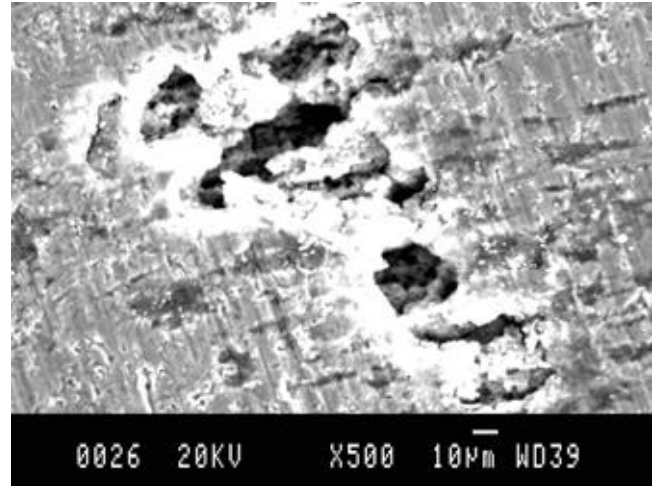


Figure 9. SEM of the sample polarized in 0.1 M Na_2SO_4 solution.

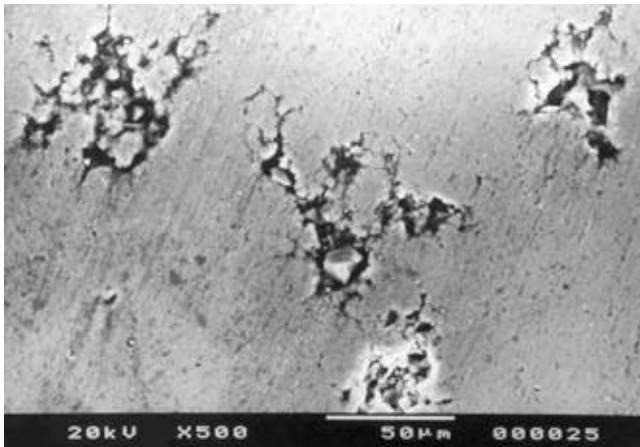


Figure 7. Micrograph of the sample immersed in 0.1 M NaNO_3 solution for 7 days.

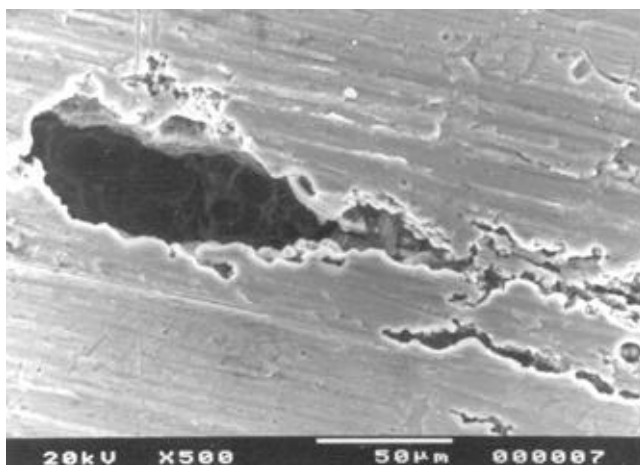


Figure 8. Micrograph of the sample immersed in 0.1 M NaCl solution for 15 days.

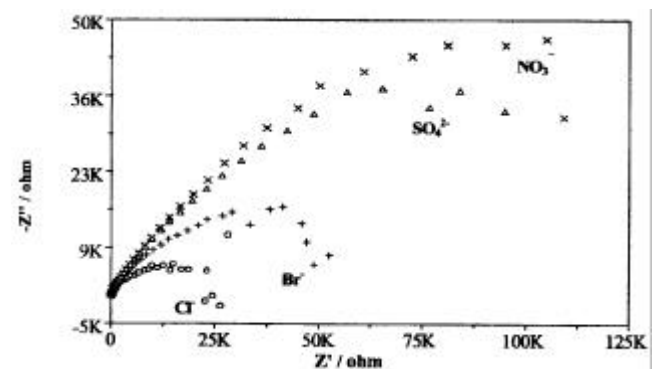


Figure 10. Nyquist plot for Al 6061 alloy in 0.1 M solution of different electrolytes.

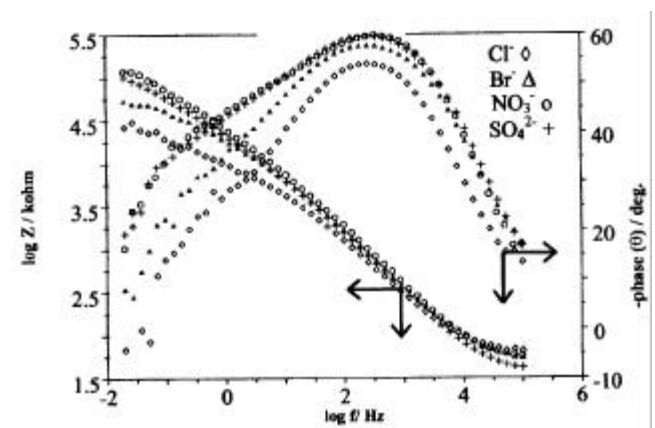
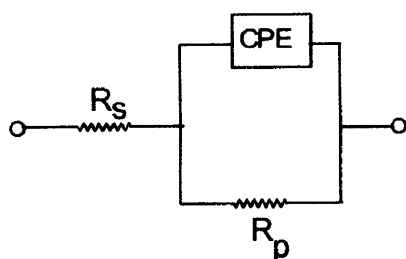


Figure 11. Bode plot for Al 6061 alloy in 0.1 M solution of different electrolytes at neutral pH.

Table 4. Equivalent circuit parameters for the 6061 Al alloy in different electrolytic media at neutral pH 25°C.

EC parameters	Cl ⁻	Br ⁻	NO ₃ ⁻	SO ₄ ²⁻
R_s (ohm)	46.90	35.90	35.9	26.62
R_p (kohm)	22.14	51.30	134.40	108.20
CPE	0.15 E-7	0.16 E-7	0.15 E-7	0.20 E-7
n	0.61	0.63	0.64	0.64

**Figure 12.** Equivalent circuit diagram.

The results show that the charge transfer process is more facile in presence of Cl⁻ than in presence of other anions. Earlier reports on DSC thermogram and TEM analysis may be referred to in this context. TEM analyses have identified **b**-Mg₂Si phases in the precipitation paths of these alloys (Das *et al* 1996). DSC thermograms have also indicated formation of micro-constituents of Mg₂Si, which are known to be highly reactive towards aqueous Cl⁻ solutions with the formation of MgO and SiO₂ leading to intergranular corrosion (Das *et al* 1994). The affected area of the material undergoing pitting and intergranular corrosion under influence of Cl⁻ and other ions are exhibited in the SEM images (figures 4 and 8) discussed above.

4. Conclusions

The present study on corrosion behaviour of Al 6061 alloy in presence of various electrolytes reveals the susceptibility of pitting which is aggravated in presence of chloride in the medium. It appears that the pit initiation was partially guided by the associated chemical processes and progressively induced the types of corrosion like exfoliation, cracking and others. The material is passive in sulfate containing medium but show extensive pitting when polarized beyond breakdown potential. Specific adsorption of Cl⁻ onto the interface is discernible from the EIS plots while NO₃⁻, SO₄²⁻ and Br⁻ are seen to impart passivity to the material at equivalent pH conditions. Appropriate models for impedance have also been developed to fit the experimental data and extract the parameters that characterize the corrosion process.

The suppression of corrosion rate with moderate period of immersion clearly indicates that during prolonged exposure in the medium, the corrosion behaviour of the material is controlled by the combined effect of the repair of the protecting coating as well as its destruction by the attack of the ionic species in solution. In reality, the oxygen diffuses into the matrix, forming internal oxides, which may also sometimes offset the weight loss by oxidation in open air conditions.

References

- Ambat R and Dwarakadasa E S 1994 *J. Appl. Electrochem.* **24** 911
- ASTM Standards: parts 3 and 4, Annual Book G31 1977 *Recommended practice for laboratory immersion corrosion testing of metals* (West Conshohocken, P.A.: ASTM International) p. 722
- Bohni H and Uhlig H H 1969 *J. Electrochem. Soc.* **116** 906
- Chavanin T U 1991 *Corrosion* **47** 472
- Conde A and Damborenea J de 1998 *Electrochim. Acta* **43** 849
- Das T, Bandyopadhyay S and Blairs S 1994 *J. Mater. Sci.* **29** 5680
- Das T, Munroe P R and Bandyopadhyay S 1996 *J. Mater. Sci.* **31** 5351
- Datta J, Bhattacharya C, Sarkar D and Bandyopadhyay S 2003 *J. Institution of Engineers (India)* **84** 79
- Datta J, Datta S, Banerjee M K and Bandyopadhyay S 2004 *Composite Part A: applied science and manufacturing* **35** 1003
- Fontana M G 1987 *Corrosion engineering* (Singapore: McGraw-Hill Inc)
- Greenwood N N and Earnshaw 1989 *Chemistry of the elements* (ed.) Maxwell McMillan Int. (Singapore: Pergamon Press)
- Guillaumin V and Mankowski G 2000 *Corros. Sci.* **42** 105
- Kahanda G L M K S and Tomkiewicz M 1990 *J. Electrochem. Soc.* **137** 3423
- Kotsikos G, Sutcliffe J M and Holroyd N J H 2000 *Corros. Sci.* **42** 17
- McCafferty E 2003 *Corros. Sci.* **45** 1421
- McDonald J R 1987 *Impedance spectroscopy* (New York: John Wiley and Sons)
- Metikos-Hukovic M, Babic R, Grubac Z and Brinic S 1994 *J. Appl. Electrochem.* **24** 772
- Pyun S-I, Moon S-M, Ahn S-H and Kim S-S 1999 *Corros. Sci.* **41** 653
- Stella M and Micheli De 1978 *Corros. Sci.* **18** 605
- Tomcsanyi L, Varga K, Bartik I, Horanyi G and Maleczki E 1989 *Electrochim. Acta* **34** 855